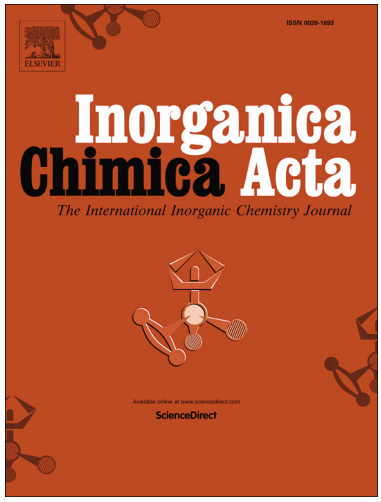

Thermal, spectroscopic studies and hydrogen bonding in supramolecular assembly of azo rhodanine complexes

A.Z. El-Sonbati, M.A. Diab, A.A. El-Bindary, G.G. Mohamed, Sh.M. Morgan

PII: S0020-1693(15)00124-3
DOI: http://dx.doi.org/10.1016/j.ica.2015.02.031
Reference: ICA 16449

To appear in: *Inorganica Chimica Acta*

Received Date: 26 December 2014
Revised Date: 25 February 2015
Accepted Date: 27 February 2015

Please cite this article as: A.Z. El-Sonbati, M.A. Diab, A.A. El-Bindary, G.G. Mohamed, Sh.M. Morgan, Thermal, spectroscopic studies and hydrogen bonding in supramolecular assembly of azo rhodanine complexes, *Inorganica Chimica Acta* (2015), doi: http://dx.doi.org/10.1016/j.ica.2015.02.031

Thermal, spectroscopic studies and hydrogen bonding in supramolecular assembly of azo rhodanine complexes

A.Z. El-Sonbati[1,+], M.A. Diab[1], A.A. El-Bindary[1], G.G. Mohamed[2], Sh.M. Morgan[1]

[1]Chemistry Department, Faculty of Science, Damietta University, Damietta, Egypt

[2]Chemistry Department, Faculty of Science, Cairo University, Giza, Egypt

Abstract

A novel series of Cu(II) complexes of azo rhodanine derivatives (HL_n) have been prepared and characterized by thermal analysis, spectral studies (IR, mass, UV-visible, ESR) and magnetic measurements. IR spectra suggest that the HL_n acts as a bidentate ligands coordinating *via* (N=N) and deprotonated enolized carbonyl oxygen (-C-O-). ESR spectra of the Cu(II) complexes show d_{x2-y2} as a ground state, suggesting tetrahedral distorted or square planar geometries around Cu(II) center. The X-ray diffraction (XRD) patterns powder forms of Cu(II) complexes shows many diffraction peaks which indicates the polycrystalline phase. Thermal properties and decomposition kinetics of compounds are investigated. The thermodynamic parameters and evaluation of kinetic parameters (E_a, ΔS^*, ΔH^* and ΔG^*) of thermal decomposition stages have been evaluated using Coast-Redfern and Horowitz-Metzger methods. Cu(II) complexes are screened for their biological activity against bacterial and fungal species. The Cu(II) complexes showed antimicrobial activities against *Staphylococcus aureus* and *Penicillium italicum*.

Keywords: Azodye complexes; ESR; Thermal properties; Thermodynamic parameters; Antimicrobial activity.

[+]Corresponding author Tel.: +201060081581; fax: +20 572403868.
E-mail address: elsonbatisch@yahoo.com (A.Z. El-Sonbati).

1. Introduction

Azodyes are an important class of organic colorants which consist of at least a conjugated chromophore azo (-N=N-) group and the largest and most versatile class of dyes. It has been known for many years that azo compounds are the most widely used class of dyes due to their versatile application in various fields such as the dyeing of textile fiber and coloring of different materials, and for plastics, biological-medical studies, and advanced applications in organic synthesis [1-4].

Over the past decades, azodyes and their transition metal complexes have made significant contribution in the development of co-ordination chemistry. The most important step in the development of metal complexes was perhaps the preparation of a new ligand which exhibit unique properties and novel reactivity. Since, the electron donor and electron acceptor properties of the ligand, structural functional groups and the position of the ligand in the coordination sphere together with the reactivity of coordination compounds may be a factor of different studies [4-6]. Azodyes metal complexes have been studied extensively [6-9] because of their attractive chemical and physical properties and their wide range of applications such as catalysts, antimicrobials and corrosion inhibitors. The presence of the nitrogen atoms of the azo group makes the azodyes more significant chemically and biologically [5,10].

Azo compound based on rhodanine, play a central role as chelating agents for a large numbers of metal ions, as they form a stable six- member ring after complexation with a metal ion and also it could be used as analytical reagents [11,12]. The complex-formation equilibrium have been reported for several kinds of rhodanine derivatives [4,13-15]. Potentiometry, conductivity and spectroscopy measurements on the coordination ability biologically important azo derivatives have shown that their complexes are very stable [16-18].

In this present study, we report the synthesis, characterization of Cu(II) complexes of azo rhodanine derivatives ligands (HL_n). The structure of the isolated complexes is elucidated using elemental analyses, IR, mass spectra, magnetic moment, ESR and thermogravimetric analysis. The activation thermodynamic parameters were calculated using Coats–Redfern and Horowitz-Metzger methods. Study of the antimicrobial activities of Cu(II) complexes.

2. Experimental

All the chemicals used were of British Drug House quality.

2.1. Synthesis of 5-(4'-derivatives phenylazo)-2-thioxothiazolidin-4-one (HL_n)

In a typical preparation, 25 ml of distilled water containing 0.01 mol hydrochloric acid were added to aniline (0.01 mol) or *p*-derivatives. To the resulting mixture stirred and cooled to 0 ºC, a solution of 0.01 mole sodium nitrite in 20 ml of water was added dropwise. The formed diazonium chloride was consecutively coupled with an alkaline solution of 0.01 mol 2-thioxo-4-thiazolidinone, in 10 ml of pyridine. The colored precipitate, which formed immediately, was filtered through sintered glass crucible, washed several times with water and ether then dried in a vacuum desiccator over P_2O_5. The elemental analyses of the ligands (HL_n) are given in Table 1.

2.2. Preparation of the complexes

$CuCl_2.2H_2O$ (0.01 mol) in 30 ml ethanol was added to a solution of HL_n (0.01 mol) in 30 ml ethanol. The mixture was then refluxed on a water bath for ~ 4 h and allowed to cool whereby the solid complexes were separated, which filtered off, washed several times with ethanol, the solid was dried in a vacuum desiccator over P_2O_5.

2.3. Biological activity investigation

For this investigation the agar well diffusion method was applied [5,10]. The antibacterial activities of the investigated compounds were tested against two local Gram positive bacterial species (*Bacillus cereus* and *Staphylococcus aureus*) and two local Gram negative bacterial species (*Escherichia coli* and *Klebsiella pneumoniae*) on nutrient agar medium. Also, the antifungal activities were tested against four local fungal species (*Aspergillus niger, Alternaria alternata, Penicillium italicum* and *Fusarium oxysporium*) on DOX agar medium. The concentrations of each solution were 150, 100 and 50 µg/ml in dimethyl formamide (DMF). By using a sterile cork borer (10 mm diameter), wells were made in agar medium plates previously seeded with the test microorganism. 200 µl of each compound was applied in each well. The agar plates were kept at 4 °C for at least 30 min to allow the diffusion of the compound to agar medium. The plates were then incubated at 37 °C or 30 °C for bacteria and fungi, respectively. The diameters of inhibition zone were determined after 24 h and 7 days for bacteria and fungi, respectively, taking the consideration of

the control values (DMF). Penicillin and miconazole were used as reference substances against bacteria and fungi, respectively.

2.4. Analytical and physical measurements

Elemental microanalyses of the separated compounds for C, H, N and S were determined on Automatic Analyzer CHNS Vario ELIII, Germany. The analyses were repeated twice to check the accuracy of the analyzed data. The ^{1}H-NMR spectra were obtained with a JEOL FX90 Fourier transform spectrometer with DMSO-d_6 as the solvent and TMS as an internal reference. The infrared spectra were recorded as KBr discs using a Perkin-Elmer 1340 spectrophotometer. Mass spectra were recorded by the EI technique at 70 eV using MS-5988 GS-MS Hewlett-Packard. X-ray diffraction analysis of complexes powder forms was recorded on X-ray diffractometer in the range of diffraction angle $2\theta^{o}$ = 4-70^{o}. This analysis was carried out using CuKα radiation (λ = 1.540598 Å). The applied voltage and the tube current are 40 KV and 30 mA, respectively. Ultraviolet-visible (UV-Vis) spectra of the compounds were recorded in nuzol solution using a Unicom SP 8800 spectrophotometer. The magnetic moment of the prepared solid complexes was determined at room temperature using the Gouy`s method. Mercury(II) (tetrathiocyanato)cobalt(II), [Hg{Co(SCN)$_4$}], was used for the calibration of the Gouy tubes. Diamagnetic corrections were calculated from the values given by Selwood [19] and Pascal's constants. Magnetic moments were calculated using the equation, $\mu_{eff.} = 2.84\ [T\chi_M^{coor.}]^{1/2}$. Thermal studies were computed on Simultaneous Thermal Analyzer (STA) 6000 system using thermogravimetric analysis (TGA) method. Thermal properties of the samples were analyzed in the temperature range from 30 to 800 °C at the heating rate of 10 ^{o}C/min under dynamic nitrogen atmosphere. ESR measurements of powdered samples were recorded at room temperature using an X-band spectrometer utilizing a 100 kHz magnetic field modulation with diphenyl picrylhydrazyle (DPPH) as a reference material. The conductance measurement was achieved using Sargent Welch scientific Co., Skokie, IL, USA.

3. Results and discussion

3.1. Stoichiometry of the copper(II) complexes

The stoichiometry of the complexes have been deduced from their elemental analysis (Table 2), which indicates that the metal complexes fall into 1:1 (monomeric) (metal:ligand). The ligands (HL_n) are mononucleating and hence require one metal

ion for coordination. All the products were partially soluble in common organic solvents. Microanalytical data are in good agreement with stoichiometry proposed for complexes (Table 2). The elemental analysis correspond to the general formula $[Cu(L_n)(OH_2)Cl].nH_2O$ for all complexes. The principle HL_n ligands undergoes mono deprotonation to form L_n in Cu(II) complexes and acts as a bidentate ligand occupying two positions of an geometrical structure. The formation of the complexes may be represented by the following reaction:

$$CuCl_2.2H_2O + HL_n \rightarrow [Cu(L_n)(OH_2)Cl].nH_2O + HCl$$

where L_n represents the anion of HL_n

3.2. Molar conductance of the complexes

The molar conductance of 10^{-3} M of solutions of the Cu(II) complexes in DMSO is calculated at 25 ± 2 ^{o}C. It is concluded from the results that Cu(II) chelates under investigation were found to have molar conductance values of the compounds (1:1)(M:L_n) shows that they are non-electrolytic. This indicates that the anions are involved in the coordination sphere [18]. This is in accordance with the fact that conductivity values for a non-electrolyte are below 50 Ω^{-1} mol^{-1} cm^2 in DMSO solution [8,14]. Such a non-zero molar conductance value for each of the complex in the present study is most probably due to the strong donor capacity of DMSO, which may lead to the displacement of anionic ligands and change of electrolyte type [18].

3.3. Infrared spectra and nature of coordination

The infrared spectra of ligands (HL_n) give interesting results. The broad absorption band located at ~3400 cm^{-1} is assigned to υ(OH). The low frequency bands indicate that the hydroxyl hydrogen atom is involved in keto ↔ enol tautomerism through hydrogen bonding (A↔B, Fig. 1). The two bands located at 1330 and 1370 cm^{-1} are assigned to in-plane deformation and the band at 1130 cm^{-1} is due to υ(C–OH) (Fig. 1-C). The ligands give two bands at ~3200–3040 cm^{-1} which can assigned to asymmetric and symmetric stretching vibrations of N–H group and intramolecular hydrogen bonding NH···O systems (Fig. 1-D), respectively. However, if such a mechanism is taking place in case of intermolecular hydrogen bond, the OH···O and OH···N bond distances differ (Fig. 1-E and 1-F, respectively).

By comparing the infrared spectra of the free ligands to that of the prepared complexes the following points are observed:

1. The appearance of a new bands around ~3360 cm^{-1} and two sharp bands at ~715 and 430 cm^{-1}, the latter two can be assigned to the wagging and rocking modes of vibration of the water molecule, respectively, [14,18] in the prepared complexes (**1-5**) may be taken as a strong evidence for the presence of coordinated water.

2. In the IR spectra of all the ligands, the band at ~1535 cm^{-1} due to the υ(–N=N–) mode is observed. In the metal chelates, this frequency is lowered by 10–25 cm^{-1} indicating the bonding of the azo nitrogen to the copper atom. The υ(C–N) vibration appearing at ~1480 cm^{-1} in the ligands suffers a downward shift of ~10 cm^{-1}, thereby supporting the assumption that the copper ion is coordinated to one of the azo nitrogen atoms.

3. Further proof for the involvement of both enol oxygen and azodye-nitrogen atoms in complexation is the appearance of weak bands in the complexes in the range of 465-500 and 430-445 cm^{-1} due to υ(Cu-O) and υ(Cu-N), respectively, [7,14] which are absent in the free ligands.

According to the structure as shown in Fig. 2, the ligand (HL_n) takes its usual anionic form (L_n) to chelate Cu(II) through N- of azo group and oxygen atom of enol group (Fig. 1-C).

3.4. ^{1}H NMR spectra

The ^{1}H NMR spectra of azo rhodanine and its derivatives show signal for CH (~ 4.42 ppm), favoring formation of an intramolecular hydrogen bond with the N=N (azodye) group. Electron-withdrawing substituents reduce the intramolecular hydrogen bond as indicated by the marked shift of the hydroxyl signal to higher field in the *p*-NO_2 compounds. Electron-donating substituents give the opposite effect, arising from the increasing basicity of the azonitrogen. The broad signals assigned to the OH protons at ~11.36–11.88 ppm are not affected by dilution. The previous two protons disappear in the presence of D_2O. Absence of –CH proton signal of the ligand moiety indicated the existence of the ligands in the azo-enol form. According to El-Sonbati et al. [5-9], hydrogen bonding leads to a large deshielding of the protons. The shifts are in the sequence: *p*-(NO_2 > H > OCH_3). In the meantime, the ^{1}H NMR of the HL_1 exhibits signals at δ(ppm) [3.9 (s, 3H, OCH_3)]. The aromatic protons have resonance at 7.10–7.45 ppm for the ligands. The chemical shifts, δ, ppm owing to NH proton (of rhodanine) remain practically unchanged in the complexes, indicating that

(NH of rhodanine) nitrogen does not involved in ligands coordination to the metal. Absence of CH proton signal of the rhodanine azo moiety indicated the existence of the ligands in the azo-enol form.

3.5. Mass spectra

The electron impact mass spectra of Cu(II) complexes **(2-5)** are recorded and investigated at 70 eV of electron energy. The mass spectra of the studied Cu(II) complexes are characterized by moderate to high relative intensity molecular ions peaks at 70 eV. It is obvious that, the molecular ion peaks are in good agreement with their suggested empirical formula as indicated from elemental analyses (Table 2). The mass spectral fragmentation mode of Cu(II) complex **(3)** (Fig. 3) shows the exact mass of 353, corresponding to the formula [$CuC_9H_6N_3OS_2Cl$ (OH_2)]. The ion of m/z = 353 undergoes fragmentation to a stable peak at m/z = 237 by losing chlorine atom, water molecule and copper ion (structure **I**) as shown in scheme 1. The loss of C_2HNOS molecule leads to the fragmentation with m/z = 150 (structure **II**). The loss of sulpher atom leads to the fragmentation with m/z = 118 (structure **III**). A breakdown of the backbone of complex **(3)** gives the fragments **(IV)** and **(V)**. The mass spectra of Cu(II) complexes **(2, 4** and **5)** gives mass peaks at 385, 405 and 416, respectively, corresponding to the formulae [$CuC_{10}H_8N_3OS_2Cl$ (OH_2)]H_2O, [$CuC_9H_5N_3OS_2Cl_2$ (OH_2)]H_2O and [$CuC_9H_5N_4O_3S_2Cl$ (OH_2)]H_2O as shown in Figures S1, S2 and S3, respectively, in the supplementary. The stable fragmentation of the mass spectra of the complexes is in good agreement with the proposed molecular formula for these complexes.

3.6. X-ray diffraction

Single crystals of the complexes could not be prepared to get the XRD and hence the powder diffraction data were obtained for structural characterization. Structure determination by X-ray powder diffraction data has gone through a recent surge since it has become important to get to the structural information of materials, which do not yield good quality single crystals.

The X-ray diffraction (XRD) patterns powder forms of Cu(II) complexes (**2-4**) are presented in Fig. 4. The XRD of Cu(II) complexes (**2-4**) shows many diffraction peaks which indicates the polycrystalline phase. The average crystallite size (ξ) can be calculated from the XRD pattern according to Debye-Scherrer equation [20,21]:

$$\xi = \frac{K\lambda}{\beta_{1/2}\cos\theta}. \qquad (1)$$

The equation uses the reference peak width at angle (θ), where λ is wavelength of X-ray radiation (1.541874 Å), K is constant taken as 0.95 for organic compounds [21] and $\beta_{1/2}$ is the width at half maximum of the reference diffraction peak measured in radians. The dislocation density,δ, is the number of dislocation lines per unit area of the crystal. The value of δ is related to the average particle diameter (ξ) by the relation [22]:

$$\delta = \frac{1}{\xi^2}. \qquad (2)$$

The values of ξ are calculated and found to be 210, 267 and 316 nm for complexes **(2)**, **(3)** and **(4)**, respectively. The values of δ are 2.27×10^{-5}, 1.40×10^{-5} and 1.00×10^{-5} nm^{-2} for complexes **(2)**, **(3)** and **(4)**, respectively.

3.7. Magnetic moment and electronic spectra

The magnetic moment of all the Cu(II) complexes at room temperature lie in the range 1.84-1.94 B.M. corresponding to one unpaired electron [23]. This indicates that these complexes are monomeric in nature and the absence of metal-metal interaction. This behavior suggest square planar geometry for the Cu(II) complexes [24]. The electronic spectra of complexes (**1**-**5**) showed two weak, low energy bands in the region of 14980-15260 and 20865-21290 cm^{-1}, respectively, which may be assigned to $^2B_{1g} \rightarrow {}^2A_{1g}$ and $^2B_{1g} \rightarrow {}^2Eg$ transitions in a distorted square planar ligands field [25].

3.8. ESR spectra

The spin Hamiltonian parameters of the complexes were calculated and presented in Table 3. In axial symmetry the g-values are related by the expression $G = (g_{ll}-2)/(g_{\perp}-2) = 4$, where G is the exchange interaction parameter. According to Hathaway and Billing [26], if the value of G is greater than 4, the exchange interaction between Cu(II) centers in the solid state is negligible, whereas when is less than 4, considerable exchange interaction is indicated in the solid complex. The observed value for the exchange interaction parameter for the complex **(1)** (G = 3.1) suggests the significant exchange coupling is present and the misalignment is appreciable, and the unpaired electron is present in the d_{x2-y2} orbital. This result also indicates that the exchange coupling effects are not operative in the present complex. The tendency of A_{ll} to decrease with an increase of g_{ll} is an index of an increase of the

tetrahedral distortion in the coordination sphere of copper. In order to quantify the degree of distortion of the Cu(II) complexes. We selected the f factor g_{II}/A_{II} obtained from the ESR spectra. Although the factor, which is considered as an empirical index of tetrahedral distortion [27]. Its value ranges between 105 and 135 for square planar complexes, depending on the nature of the coordinated atoms. In the presence of a tetrahedral distorted structure the values can be much larger [9]. For all copper(II) complexes the g_{II}/A_{II} quotient is demonstrating the presence of significant dihedral angle distortion in the xy-plane and correlate well with the tetrahedral distortion from square planar geometry arrangement around copper center. In a square planar Cu(II) complex, the unpaired electron residue in the d_{x2-y2} orbital giving $^2B_{1g}$ as the ground state with g_{II} and $g_{\perp}$ are given in the order $g_{II} > g_{\perp} > 2$, while the unpaired electron lies in the d^2z orbital giving $^2A_{1g}$ as the ground state with $g_{\perp} > g_{II} > 2$.

As shown in Table 3, the values of g_{II}, α^2 and K_{II}^2 are related to the nature of the *p*-substituent as they increase according to the following order *p*-(NO_2 > H > OCH_3). This can be attributed to the fact that the effective charge increased due to the electron withdrawing *p*-substituent in complex **(5)** while it decreased by the electrons donating character of complex **(1)**. This is in accordance with that expected from Hammett's constant (σ^R) as shown in Fig. 5, correlate the values of g_{II}, α^2 and K_{II}^2 with σ^R it is clear that all these values increase with increasing σ^R.

Significant information about the nature of bonding in the Cu(II) complexes can be derived from the relative magnitudes of K^2_{II} and $K^2_{\perp}$. In the case of pure σ-bonding, $K^2_{II} \approx K^2_{\perp} = 0.77$, whereas $K^2_{II} < K^2_{\perp}$ implies considerable in-plane π-bonding, while for out-of plane π-bonding $K^2_{II} > K^2_{\perp}$. Molecular orbital coefficients α^2 (in-plane σ-bonding), β^2 (in-plane π-bonding) and γ^2 (out-plane π-bonding) were calculated. The α^2 values for the present copper complexes lie in the range of 0.58-0.72 supporting the covalent nature of these complexes (Table 3). The observed β^2 values (1.03, 1.00 and 0.91) and γ^2 values (0.96, 1.01 and 1.17) shows that there is interaction in the out-of-plane π-bonding, whereas the in-plane π-bonding is predominantly ionic. This is also confirmed by orbital reduction factors [28] which were estimated from the simple relations. For the present complexes, the observed order $K^2_{\perp} > K^2_{II}$ implies a greater contribution from in-plane π-bonding than for out-of-plane π-bonding in metal-ligand π-bonding. Thus, the ESR study of the copper complexes has provided supporting evidence for the optical results. We found that the values of K_{II}^2 and $K_{\perp}^2$ increase with increasing g_{II} and $g_{\perp}$ as shown in Fig. 6.

3.9. Thermogravimetric analysis study

The Thermogravimetric analysis (TGA) curves for the ligands (HL_n) (where n = 1, 3 and 5) and their Cu(II) complexes **(1, 3** and **5)** are shown in Figs. 7 and 8. For HL_1 and HL_3 there are two stages of the loss of masses, while for HL_5 there are three stages [17]. The first degradation stage for ligand (HL_1) takes place in the range of 200-320 ^oC was corresponding to the loss of $C_3H_2S_2N_3O$ molecule, representing a weight loss of 61.90% and its calculated value was 59.93%. The second degradation stage takes place in the range of 320-655 ^oC was corresponding to the loss of C_7H_7O molecule, representing a weight loss of 38.10 % and its calculated value was 40.07%.

In HL_3 ligand, the first degradation stage takes place in the range of 145-400 ^oC was corresponding to the loss of $C_3H_2S_2N_2O$ molecule, representing a weight loss of 59.80% and its calculated value was 61.60%. The second degradation stage takes place in the range of 400-655 ^oC was corresponding to the loss of C_6H_5N molecule, representing a weight loss of 39.90% and its calculated value was 38.39%.

On the other hand, the first degradation stage in the range of 30-112 ^oC for ligand (HL_5) was corresponding to the loss of solvent molecule [17]. The second degradation stage takes place in the range of 112-284 ^oC was corresponding to the loss of $C_3H_2S_2$ molecule, representing a weight loss of 35.60% and its calculated value was 36.17%. The third degradation stage takes place in the range of 284-640 ^oC was corresponding to the loss of $C_6H_4N_4O_3$ molecule, representing a weight loss of 58.70% and its calculated value was 63.83%.

The TGA curves of Cu(II) complexes are taken as a proof for the existing of water molecule as well as the anions to be coordination sphere. The temperature intervals and the percentage of loss of mass are listed in Table 4. The first stage of decomposition in the range ~30-80 ºC for Cu(II) complexes can be attributed to loss of lattice water molecule [7,18] (Fig. 8). The second stage of decomposition corresponds to the loss of coordinated water molecule, HCl molecule and decomposition of a part of the ligand. The third stage of decomposition is due to decomposition of a part of ligand leaving copper oxide as a residue. The third stage is attributed to loss of a part of the ligand. The final weight losses are due to the decomposition of the rest of the ligand leaving copper oxides residue (Table 4).

3.10. Kinetic studies

The kinetic parameters such as activation energy (E_a), enthalpy (ΔH^*), entropy (ΔS^*), and Gibbs free energy change of the decomposition (ΔG^*) are evaluated

graphically by employing the Coast-Redfern [29] and Horowitz-Metzger [30] methods. The thermodynamic data obtained with the two methods for the decomposition stages for Cu(II) complexes (**1**, **3** and **5**) are in harmony with each other as shown in Table 5 and Figures 9 and 10. The kinetic data obtained from the two methods are comparable and can be considered in good agreement with each other.

The high values of the energy of activation (E_a) of the complexes reveal the high stability of such chelates due to their covalent bond character [31]. The relation between E_a and Hammett's substituent coefficients (σ^R) for Cu(II) complexes (**1**, **3** and **5**) is shown in Fig. 11. It is obvious that the values of E_a for Cu(II) complexes (**1**, **3** and **5**) increase with increasing σ^R, attributable to the fact that the effective charge experienced by the d-electrons.

The entropy of activation was found to be negative values in the Cu(II) complexes (**1**, **3** and **5**) which indicates more ordered activated complex than the reactants or the reaction is slow [20,32]. The positive sign of ΔG^* for the investigated complexes reveals that the free energy of the final residue is higher than that of the initial compound, and all the decomposition stages are non-spontaneous processes. ΔS^* significantly from one stage to another which overrides the values of ΔH^* [33].

The effect of the substituents on Gibbs free energy (ΔG^*) can be confirmed in terms of Hammett's substituent coefficients (σ^R) are shown in Fig. 12. It was found that the values of ΔG^* for Cu(II) complexes (**1**, **3** and **5**) increase with increasing σ^R, attributed to the fact that the effective charge experienced by the d-electrons increases due to the electron withdrawing *p*-substituent NO_2 while it decreases by the electron donating character of OCH_3.

3.11. Antimicrobial studies

Antibacterial and antifungal activities of Cu(II) complexes (**1-5**) were tested against the Gram positive bacteria as *S. aureus* and *B. cereus*, Gram negative bacteria as *E. coli* and *K. pneumoniae* and fungal species (*A. niger*, *F. oxysporium*, *P. italicum* and *A. alternata*). The antimicrobial studies data reveal that the values of inhibition clear zone for Cu(II) complexes are related to the nature of the *p*-substituent.

The results of the antibacterial activity of Cu(II) complexes (**1**-**5**) were listed in Table 6. The Cu(II) complexes (**1**-**5**) have no antibacterial activity against *B. cereus, E. coli* and *K. pneumonia* and have low antibacterial activity against *S. aureus*. It was

found that the complex (**5**) was more potent antibacterial activity than the other complexes against *S. aureus* at high concentration (Table 6).

The results of the antifungal activity of the Cu(II) complexes (**1**-**5**) were listed in Table 7. It was found that the Cu(II) complexes (**1**-**5**) have no antifungal activity against *A. niger*, *F, oxysporum* and *A. alternata* but high antifungal activity against *P. italicum.* From these results it is observed that the complex (**5**) is more potent antifungal than the other complexes against *P. italicum.*

4. Conclusion

Spectroscopic studies of the complexation of metal ions with an azo dye showed that the absorption maxima of the complexes are bathochromically shifted compared with azo dyes. Five mononuclear copper(II) complexes have been synthesized by thermal reaction between $CuCl_2.2H_2O$ and monobasic NO bidentate azodye namely: 5-(4'-methoxyphenylazo)-2-thioxo-4-thiazolidinone (HL_1), 5-(4'-methylphenylazo)-2-thioxo-4-thiazolidinone (HL_2), 5-(phenylazo)-2-thioxo-4-thiazolidinone (HL_3), 5-(4'-chlorophenylazo)-2-thioxo-4-thiazolidinone (HL_4) and 5-(4'-nitrophenylazo) -2-thioxo-4-thiazolidinone (HL_5), respectively. The novel complexes were fully characterized by physicochemical and spectroscopic methods. Characterization of the novel complexes have shown that, the Cu(II) formed square planar complexes with 1:1 (metal:ligand) stoichiometry. IR and thermal studies indicated that the fourth position would be occupied by a water molecule and chloride ion in complexes. The thermal analysis of the ligands (HL_n) and thier Cu(II) complexes was studied by TGA technique to give more information on the structure of the investigated complexes. The thermodynamic parameters of the decomposition reaction were evaluated and discussed. It was found that the change of substituent affects the thermal properties of Cu(II) complexes. The tested complexes have good antibacterial activity against *S. aureus* and have low antifungal activity against *A. niger*, *F. oxysporium* and *A. alternata*. It was found that the complex **(5)** is more active than other complexes against *S. aureus* and *P. italicum.*

Acknowledgement

The authors would like to thank Prof. Dr. M.I. Abou-Dobara and Miss. N.F. Omar Botany Department, Faculty of Science, Damietta University, Egypt for their help during testing antimicrobial activity.

Appendix A: Supplementary material

See the attached file.

Table 1

Elemental analysis (C, H, N and S) and physical data of the ligands (HL_n).

Compound[a]	Color	Yield (%)	m.p. (°C)	Experimental (calc.) (%)			
				C	H	N	S
HL_1	Red	37.45	221	44.82 (44.93)	3.25 (3.39)	15.85 (15.72)	23.65 (23.97)
HL_2	Dark Orange	47.81	231	47.88 (47.79)	3.76 (3.61)	16.61 (16.72)	25.23 (25.50)
HL_3	Pale Yellow	42.19	237	45.68 (45.55)	2.80 (2.97)	17.85 (17.71)	26.78 (27.00)
HL_4	Light Orange	51.37	248	39.65 (39.78)	2.35 (2.23)	15.58 (15.46)	23.24 (23.57)
HL_5	Dark Yellow	66.09	245	38.42 (38.29)	2.25 (2.14)	19.98 (19.85)	22.55 (22.70)

[a]The analytical data agree satisfactory with the expected formulae represented as given in structures HL_1-HL_5. Air-stable, colored, insoluble in water, but soluble in hot ethanol, and soluble in coordinating solvents.

Table 2

Elemental analysis data of Cu(II) complexes[a] (for molecular structure see Fig. 2)[b].

Complex[c]	Experimental (calc.) (%)				
	C	H	N	S	Cl
$[Cu(L_1)(OH_2)Cl]$ **(1)**	31.14 (31.33)	2.45 (2.61)	10.76 (10.97)	16.44 (16.71)	9.11 (9.27)
$[Cu(L_2)(OH_2)Cl]H_2O$ **(2)**	31.04 (31.17)	2.52 (2.60)	10.66 (10.91)	16.44 (16.62)	9.01 (9.22)
$[Cu(L_3)(OH_2)Cl]$ **(3)**	30.46 (30.59)	2.16 (2.27)	11.67 (11.90)	18.02 (18.13)	9.88 (10.06)
$[Cu(L_4)(OH_2)Cl]H_2O$ **(4)**	26.59 (26.63)	1.66 (1.73)	10.06 (10.36)	15.52 (15.78)	16.89 (17.51)
$[Cu(L_5)(OH_2)Cl]H_2O$ **(5)**	25.83 (25.96)	1.55 (1.68)	13.13 (13.46)	15.19 (15.38)	8.42 (8.53)

[a]Microanalytical data as well as metal estimations are in good agreement with the stoichiometry of the proposed complexes, air stable, non-hydroscopic, high melting temperature and colored, [b]The excellent agreement between calculated and experimental data supports the assignment suggested in the present work, [c] L_n are the anions of the ligands (HL_n).

Table 3
ESR spectral and bonding parameters of Cu(II) complexes

Complex[a]	g_{II}	$g_{\perp}$	$g_{av.}$	G	α^2	A_{II}[b]	f	β^2	γ^2	K_{II}^2	$K_{\perp}^2$
(1)	2.268	2.064	2.132	4.1	0.58	138	164	1.03	0.96	0.58	0.59
(3)	2.270	2.070	2.137	4.0	0.61	123	184	1.00	1.01	0.61	0.62
(5)	2.288	2.094	2.159	3.1	0.72	131	174	0.91	1.17	0.66	0.84

[a]Numbers as given in Table 2.
[b]A values in 10^{-4} cm^{-1}.

Table 4

Thermal analysis data of Cu(II) complexes (**1, 3** and **5**).

Complex[a]	Temp. range (ºC)	Found mass loss (calc.) (%)	Assignment
(1)	30-225	27.51 (27.54)	Loss of coordinated H_2O molecule + HCl molecule + decomposition of a part of the ligand (C_3HN).
	225-350	18.33 (18.79)	Decomposition of a part of the ligand (C_2H_2NS).
	350-800	28.73 (29.76)	Decomposition of a part of the ligand (C_4H_4NOS).
	> 800	24.93 (23.90)	CuO residue + contaminated carbon atom.
(3)	100-200	4.78 (5.09)	Loss of coordinated H_2O molecule.
	200-370	45.67 (46.87)	Loss of HCl molecule + decomposition of a part of the ligand ($C_3HN_2S_2$).
	370-800	26.53 (25.49)	Decomposition of a part of the ligand (C_6H_4N).
	> 800	23.02 (22.53)	CuO residue.
(5)	30-70	5.46 (4.33)	Loss of outer H_2O molecule.
	70-380	40.55 (40.98)	Loss of coordinated H_2O molecule + HCl molecule + decomposition of a part of the ligand ($C_3H_2NS_2$).
	380-800	35.90 (35.57)	Decomposition of a part of the ligand ($C_6H_2N_3O_2$).
	> 800	18.12 (19.12)	CuO residue.

[a]Numbers as given in Table 2.

Table 5

Kinetic parameters of Cu(II) complexes (**1, 3** and **5**).

Complex[a]	Stage	Decomp. temp. (°C)	Method	Parameter					Correlation coefficient (r)
				E_a (kJ mol^{-1})	A (s^{-1})	ΔS* (J mol^{-1} K^{-1})	ΔH* (kJ mol^{-1})	ΔG* (kJ mol^{-1})	
(1)	First	129-222	CR	83.9	2.27×10^7	-107	80.2	128	0.9834
			HM	91.3	3.88×10^8	-84	87.6	125	0.9943
	Second	222-328	CR	65.4	2.92×10^3	-184	60.9	162	0.9843
			HM	73.5	4.91×10^4	-160	68.9	157	0.9907
(3)	First	120-264	CR	64.8	2.22×10^4	-165	60.9	138	0.9894
			HM	72.6	9.63×10^5	-134	68.8	131	0.9927
	Second	264-465	CR	40.1	0.82×10^2	-243	34.8	190	0.9887
			HM	50.0	0.31×10^2	-223	44.7	187	0.9945
(5)	First	135-390	CR	29.3	1.05×10^2	-249	24.9	158	0.9982
			HM	36.4	0.90×10^2	-232	31.9	156	0.9979
	Second	390-557	CR	134	4.24×10^6	-126	128	222	0.9949
			HM	145	7.89×10^7	-101	139	215	0.9879

[a]Numbers as given in Table 2.

Decomp. temp. = Decomposition temperature

Table 6

Antibacterial activity data of Cu(II) complexes (**1-5**). The results were recorded as the diameter of inhibition zone (mm).

Complex[a]	Conc. (μg/ml)	Gram positive bacteria		Gram negative bacteria	
		Bacillus cereus	*Staphylococcus aureus*	*Escherichia coli*	*Klebsiella pneumoniae*
(1)	50	-ve	-ve	-ve	-ve
	100	-ve	-ve	-ve	-ve
	150	-ve	1	1	-ve
(2)	50	-ve	-ve	-ve	-ve
	100	-ve	2	-ve	-ve
	150	-ve	3	-ve	-ve
(3)	50	-ve	-ve	-ve	-ve
	100	-ve	-ve	-ve	-ve
	150	3	-ve	-ve	-ve
(4)	50	-ve	-ve	1	-ve
	100	-ve	3	-ve	-ve
	150	-ve	4	-ve	-ve
(5)	50	-ve	1	-ve	-ve
	100	-ve	3	-ve	-ve
	150	-ve	5	1	-ve
Penicillin	50	1	2	1	-ve
	100	3	2	3	-ve
	150	3	2	3	-ve

[a]Numbers as given in Table 2.

Table 7

Antifungal activity data of Cu(II) complexes (**1-5**). The results were recorded as the diameter of inhibition zone (mm).

Complex[a]	Conc. (µg/ml)	*Aspergillus niger*	*Fusarium oxysporum*	*Alternaria alternata*	*Penicillium italicum*
(1)	50	-ve	-ve	-ve	-ve
	100	-ve	-ve	-ve	3
	150	-ve	-ve	-ve	4
(2)	50	-ve	-ve	-ve	5
	100	-ve	-ve	-ve	3
	150	-ve	-ve	-ve	3
(3)	50	-ve	-ve	-ve	6
	100	-ve	-ve	-ve	4
	150	-ve	-ve	-ve	2
(4)	50	-ve	-ve	-ve	-ve
	100	-ve	-ve	-ve	-ve
	150	-ve	-ve	-ve	-ve
(5)	50	-ve	-ve	-ve	4
	100	-ve	-ve	-ve	5
	150	-ve	-ve	-ve	7
Miconazole	50	1	2	1	-ve
	100	3	2	3	-ve
	150	3	2	3	-ve

[a]Numbers as given in Table 2.

References

[1] C. Anitha, C.D. Sheela, P. Tharmaraj, S. Sumathi, Spectrochim. Acta A 96 (2012) 493–500.

[2] A.U. Patel, E-Journal of Chem., 6 (2009) 1247-1252.

[3] M.A. Diab, A.A. El-Bindary, A.Z. El-Sonbati, O.L. Salem, J. Mol. Struct. 1018 (2012) 176–184.

[4] M.A. Diab, A.Z. El-Sonbati, A.A. El-Bindary, G.G. Mohamed, Sh.M. Morgan, Res. Chem. Intermed. DOI: 10.1007/s11164-015-1946-0

[5] M.I. Abou-Dobara, A.Z. El-Sonbati, Sh.M. Morgan, World J. Microbiol. Biotechnol. 29 (2013) 119-126.

[6] A.Z. El-Sonbati, M.A. Diab, A.A. El-Bindary, Sh.M. Morgan, Inorg. Chim. Acta 404 (2013) 175–187.

[7] N.A. El-Ghamaz, A.Z. El-Sonbati, M.A. Diab, A.A. El-Bindary, Sh.M. Morgan, Mater. Res. Bull. 65 (2015) 293–301.

[8] A.Z. El-Sonbati, A.A. El-Bindary, M.A. Diab, S.G. Nozha, Spectrochim. Acta A 83 (2011) 490–498.

[9] M.A. Diab, A.Z. El-Sonbati, A.A. El-Bindary, A.M. Barakat, Spectrochim. Acta A 116 (2013) 428–439.

[10] S. Alghool, H.F.A. El-Halim, A. Dahshan, J. Mol. Struc. 983 (2010) 32–38.

[11] W.I. Stephen, A. Townshend, Analytica Chim. Acta 33 (1965) 257–265.

[12] G.G. Alfonso, J.L.G. Ariza1, Microchemical Journal 26 (1981) 574–585.

[13] A.A. El-Bindary, M.M. Ghoneim, A.Z. El-Sonbati, S.A. Barakat, Mon. Chim., 129 (1998) 1259–1265.

[14] A.Z. El-Sonbati, M.A. Diab, A.A. El-Bindary, Sh.M. Morgan, Spectrochim. Acta A 127 (2014) 310-328.

[15] A.Z. El-Sonbati, A.A. El-Bindary, A. El-Dissouky, T.M. El-Gogary, A.S. Hilali, Spectrochim. Acta A 58 (2002) 1623–1629.

[16] M.S. Aziz, A.Z. El-Sonbati, A.S. Hilali, Chem. Pap. 56 (2002) 305–308.

[17] N.A. El-Ghamaz, A.Z. El-Sonbati, M.A. Diab, A.A. El-Bindary, M.K. Awad, Sh.M. Morgan, Mater. Sci. Semicond. Process., 19 (2014) 150-162.

[18] A.Z. El-Sonbati, M.A. Diab, A.A. El-Bindary, A.M. Eldesoky, Sh.M. Morgan, Spectrochim. Acta A 135 (2015) 774–791.

[19] P.W. Selwood, Magnetic Chemistry, Interscience Pub. Inc., New York, 195.

[20] M.M. Ghoneim, A.Z. El-Sonbati, A.A. El-Bindary, M.A. Diab, L.S. Serag,

Spectrochim. Acta A 140 (2015) 111–131.

[21] A.A. El-Bindary, A.Z. El-Sonbati, M.A. Diab, Sh.M. Morgan, J. Mol. Liq. 201 (2015) 36–42.

[22] S. Velumani, X. Mathew, P.J. Sebastian, Solar Energy Mater. Solar Cells, 76 (2003) 359–368.

[23] F.A. Cotton, C.W. Wilkinson, Advanced Inorganic Chemistry, third ed., Interscience Publisher, New York, 1972.

[24] A.B.P. Lever, Inorganic Spectroscopy, second ed., Elsevier, Amsterdam, 1984.

[25] M.F. Iskander, L. El-Sayed, K.I. Zaki, Transition Met. Chem. 4 (1979) 225–230.

[26] B.J. Hathaway, D.E. Billing, Coord. Chem. Rev. 5 (1970) 143–207.

[27] V.T. Kasumo, Spectrochim. Acta A 57 (2001) 1649-1662.

[28] R.K. Ray, Inorg. Chim. Acta 174 (1990) 237-257.

[29] A.W. Coats, J.P. Redfern, Nature 20 (1964) 68–79.

[30] H.W. Horowitz, G. Metzger, Anal. Chem. 35 (1963) 1464–1468.

[31] T. Taakeyama, F.X. Quimn, "Thermal Analysis Fundamental and Application to Polymer Science", Join Wiley and Sons, Chichester, 1994.

[32] A.A. Frost, R.G. Pearson, "Kinetics and Mechanisms", Wiley, New-York, 1961.

[33] S.S. Kandil, G.B. El-Hafnawy, E.A. Baker, Thermochim. Acta 414 (2004) 105–113.

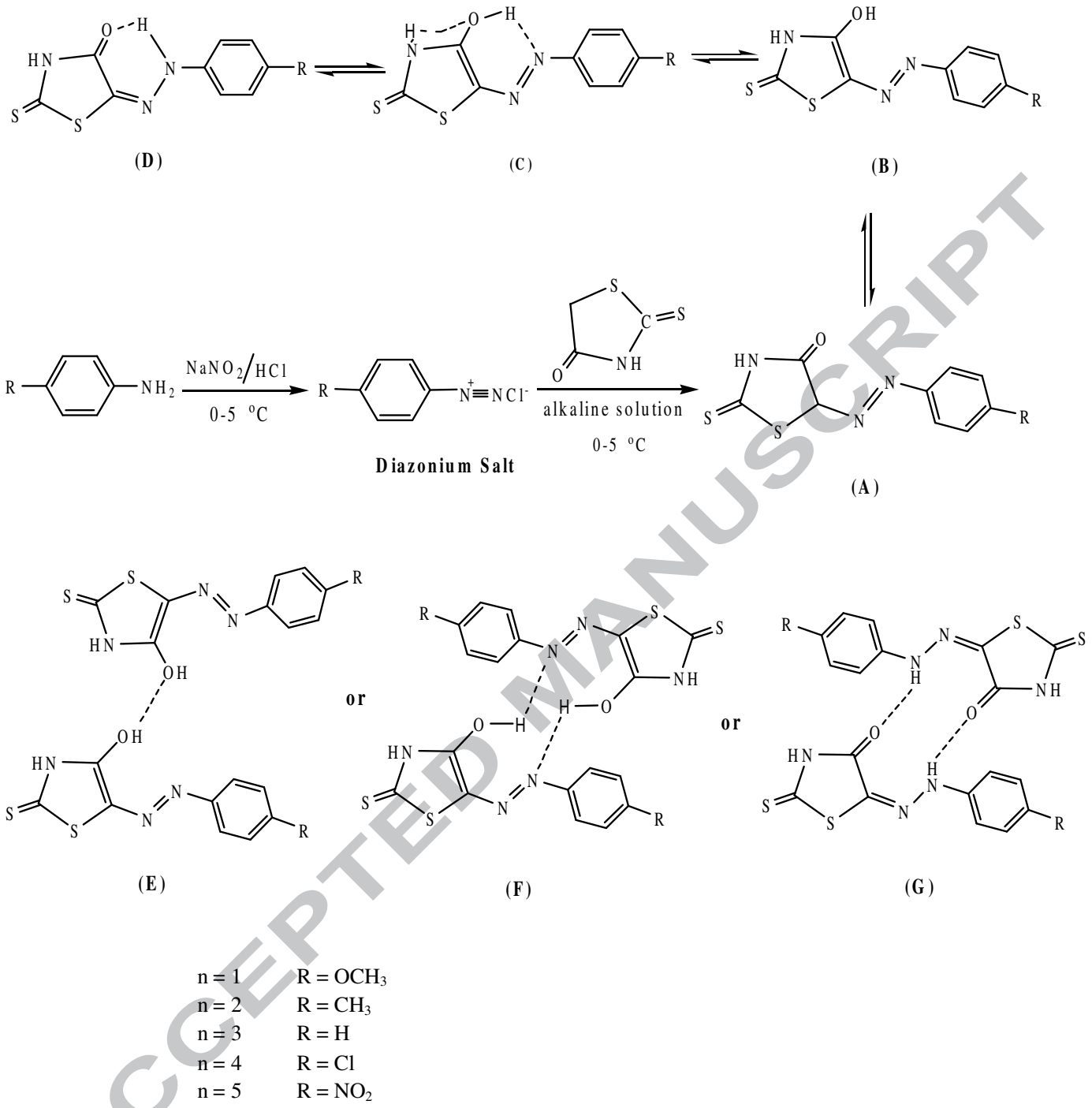

n = 1 R = OCH_3
n = 2 R = CH_3
n = 3 R = H
n = 4 R = Cl
n = 5 R = NO_2

Fig. 1. The formation mechanism and tautomeric structures of ligands (HL_n).

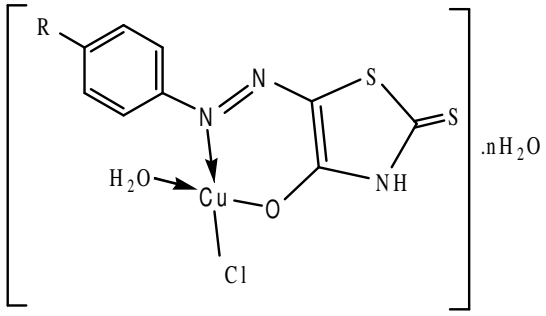

Fig. 2. The structure proposed for Cu(II)-complexes.

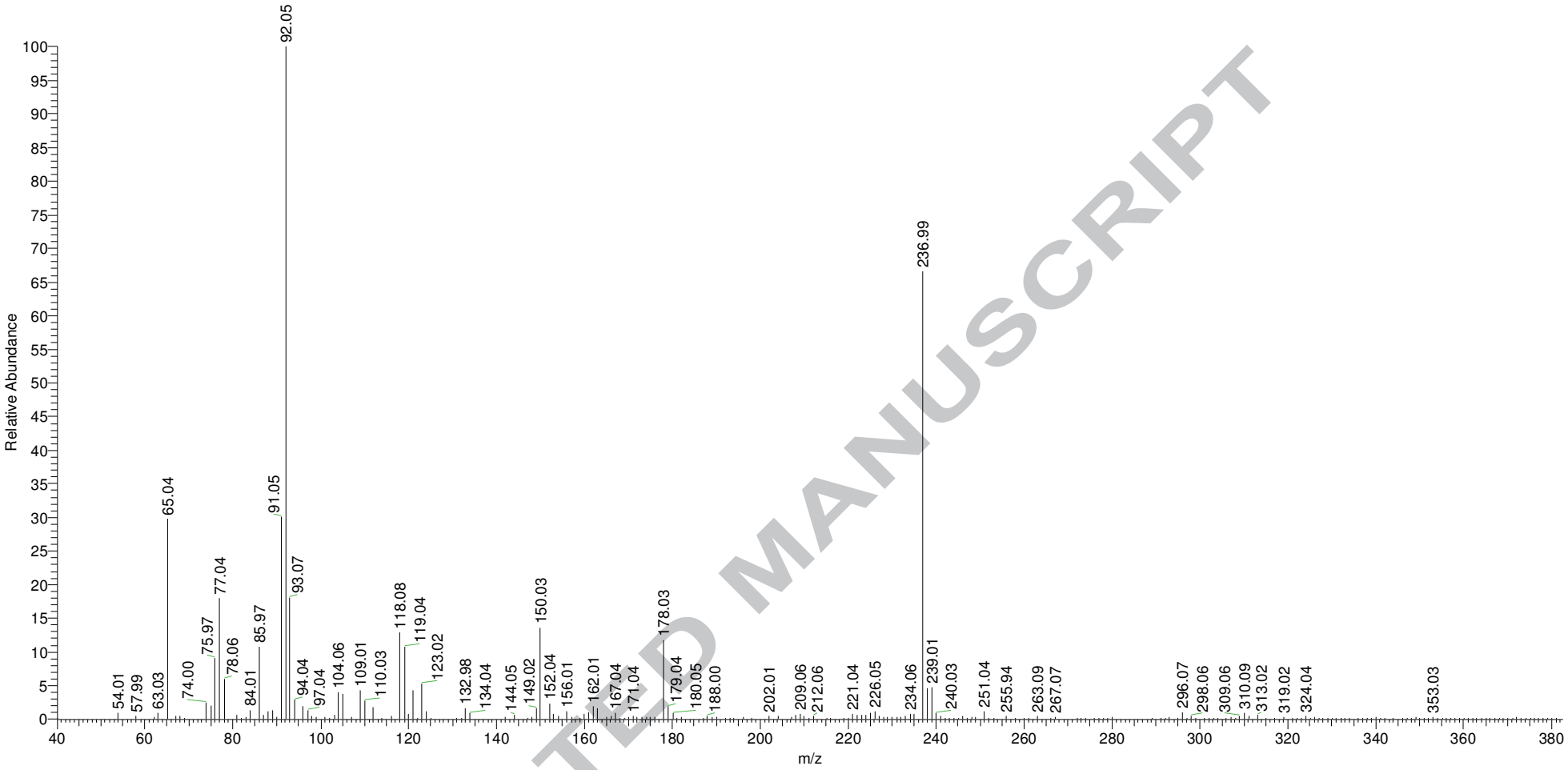

Fig. 3. Mass spectrum of $[Cu(L_3)(OH_2)Cl]$ **(3)** complex.

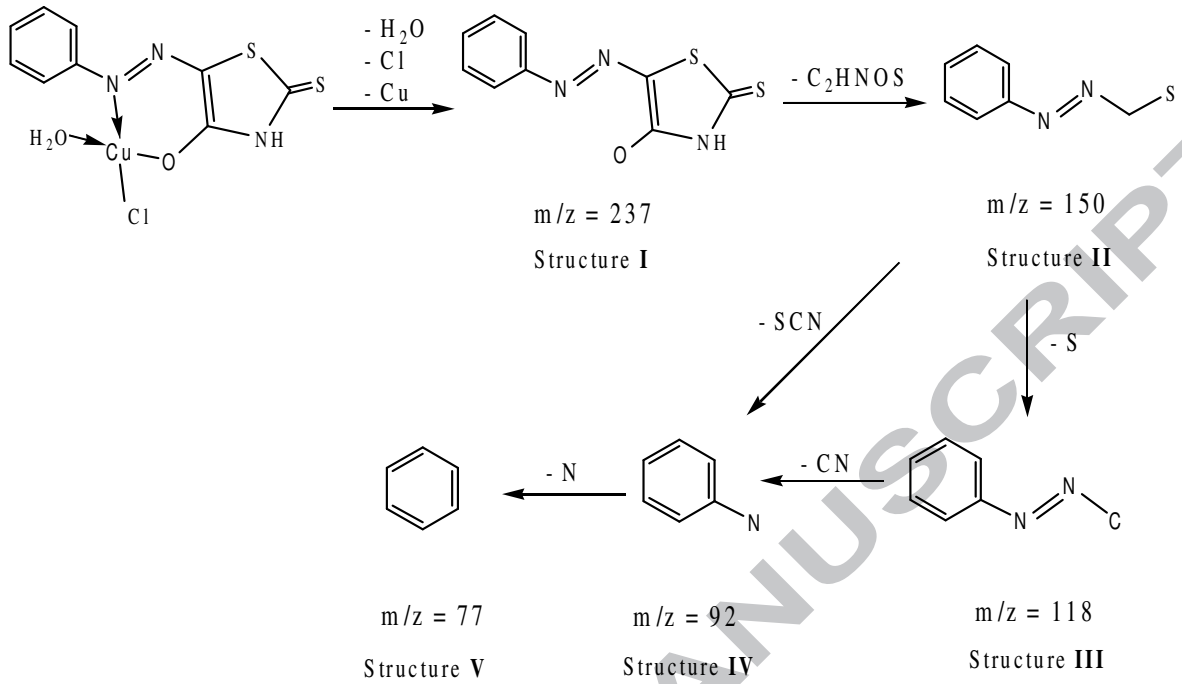

Scheme 1. Fragmentation patterns of complex **(3)**.

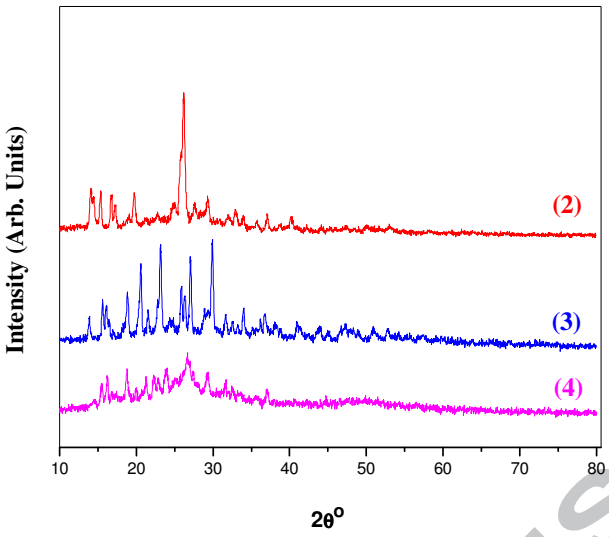

Fig. 4. X-ray diffraction patterns for powder forms of Cu(II) complexes (**2-4**).

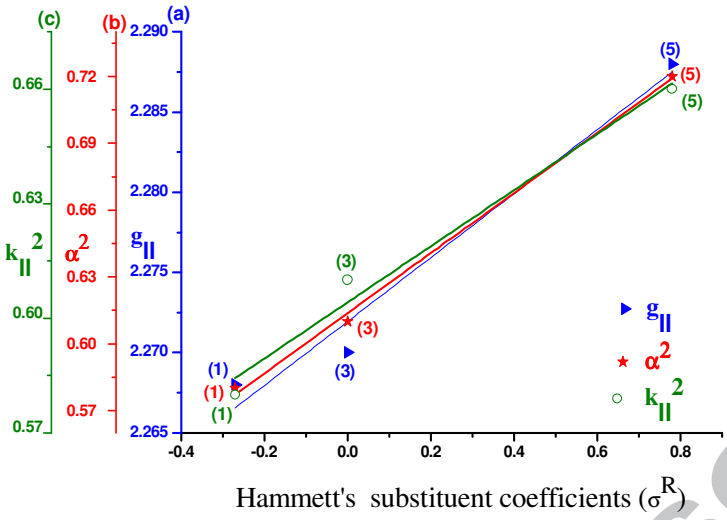

Fig. 5. The relation between Hammett's substituent coefficients (σ^R) *vs*. a) g_{II}, b) α^2 and c) K_{II}^2 of Cu(II) complexes (**1, 3** and **5**).

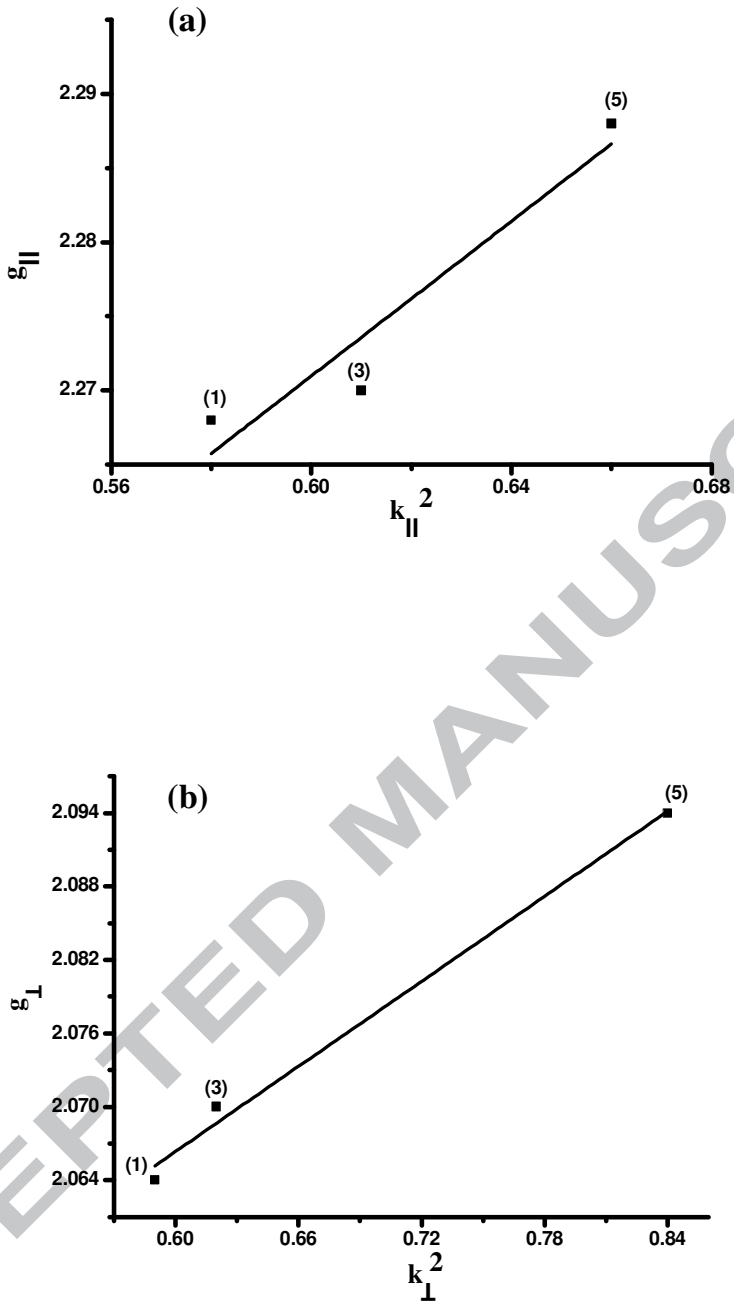

Fig. 6. The relation between a) K_{II}^2 *vs.* g_{II} and b) $K_{\perp}^2$ *vs.* $g_{\perp}$ of Cu(II) complexes (**1, 3** and **5**).

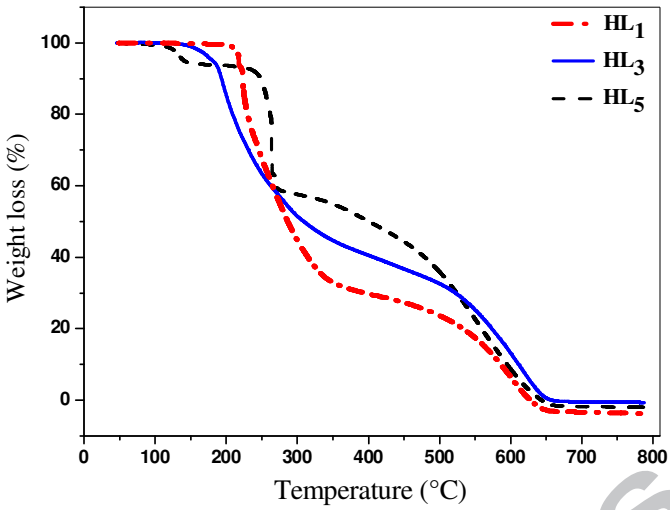

Fig. 7. TGA curve of ligands (HL_1, HL_3 and HL_5).

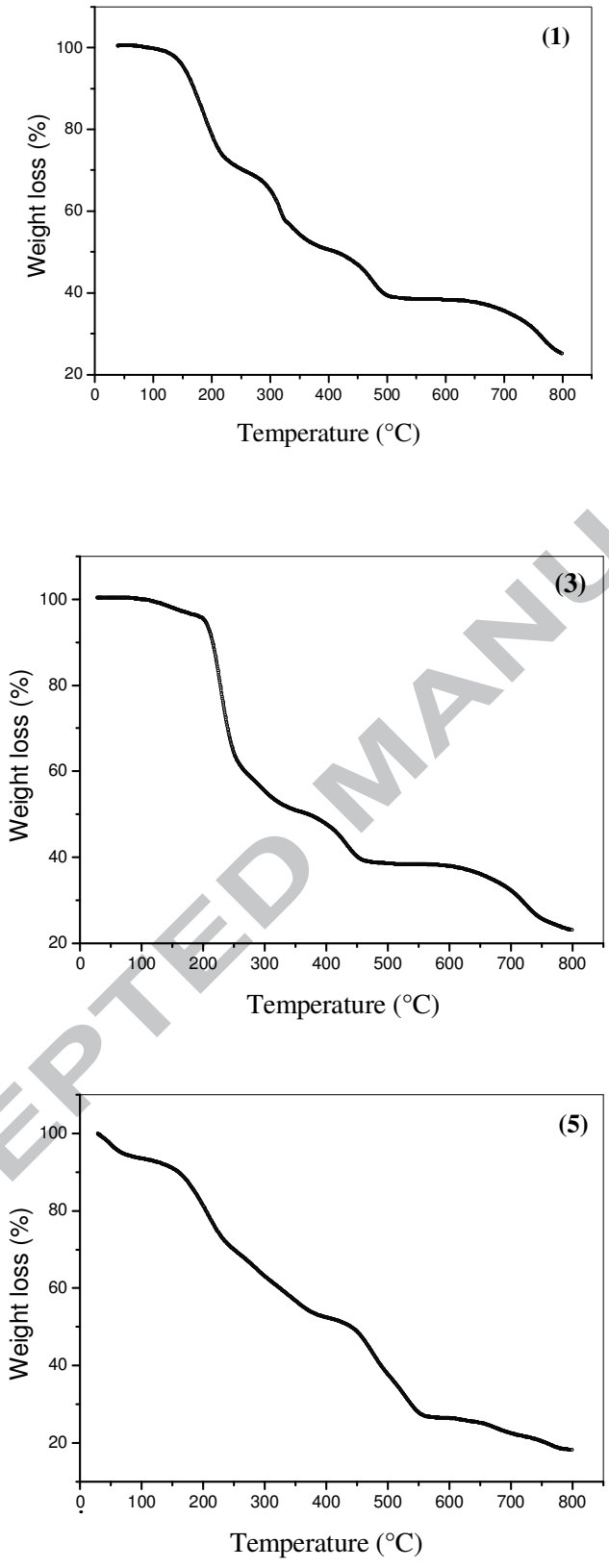

Fig. 8. TGA curves of Cu(II) complexes (**1, 3** and **5**).

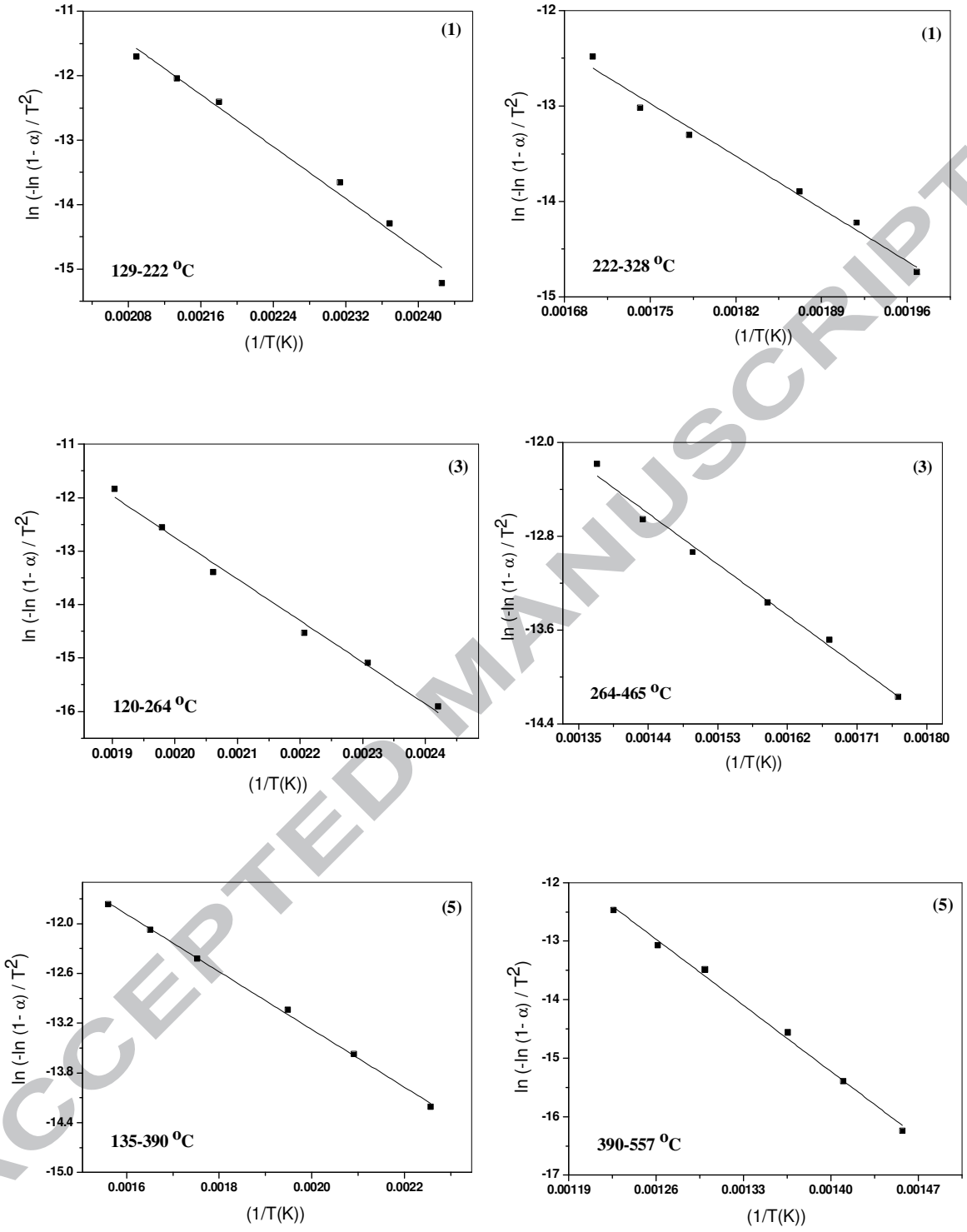

Fig. 9. Coats–Redfern (CR) of Cu(II) complexes (**1, 3** and **5**).

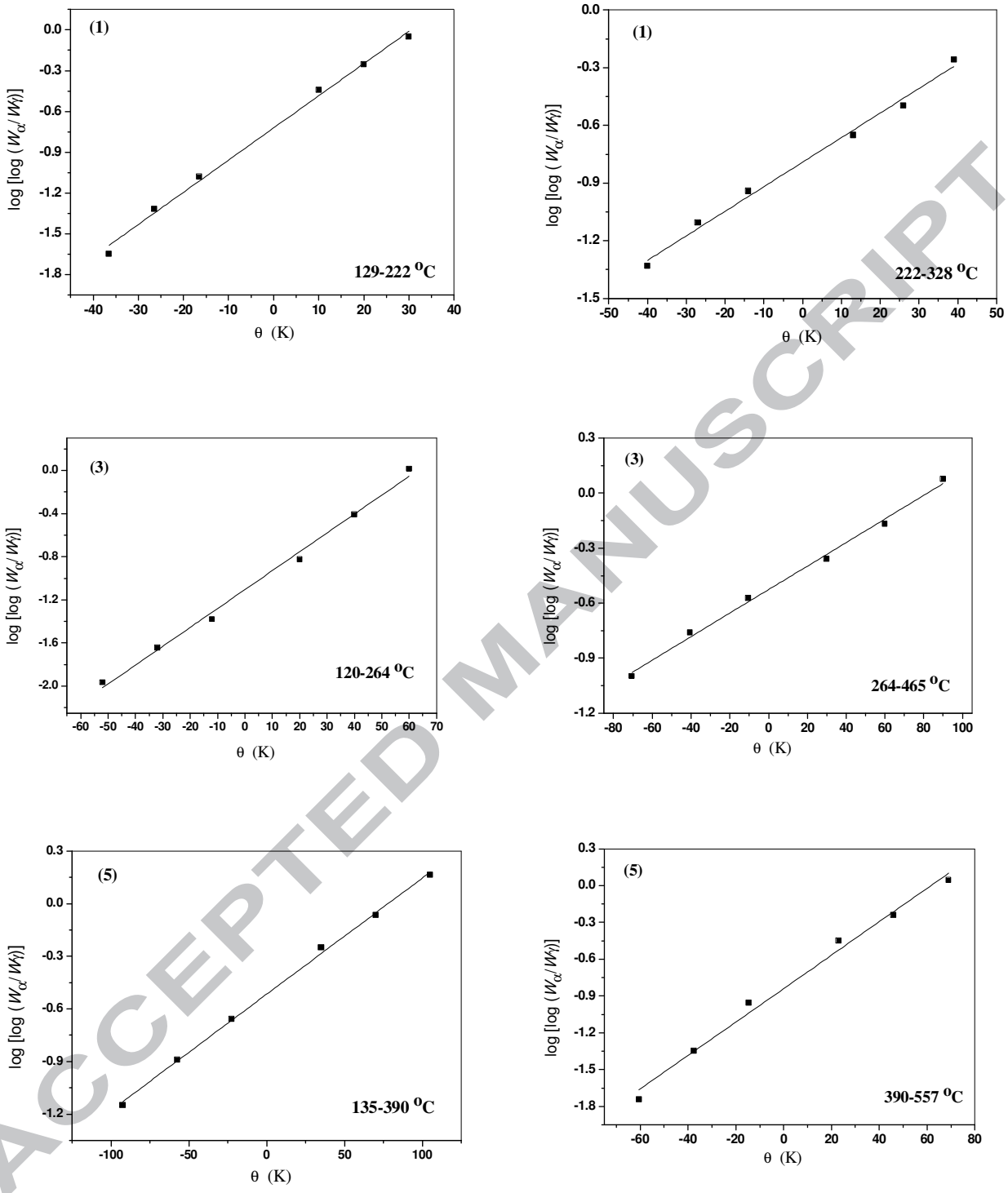

Fig. 10. Horowitz-Metzger (HM) of Cu(II) complexes (**1, 3** and **5**).

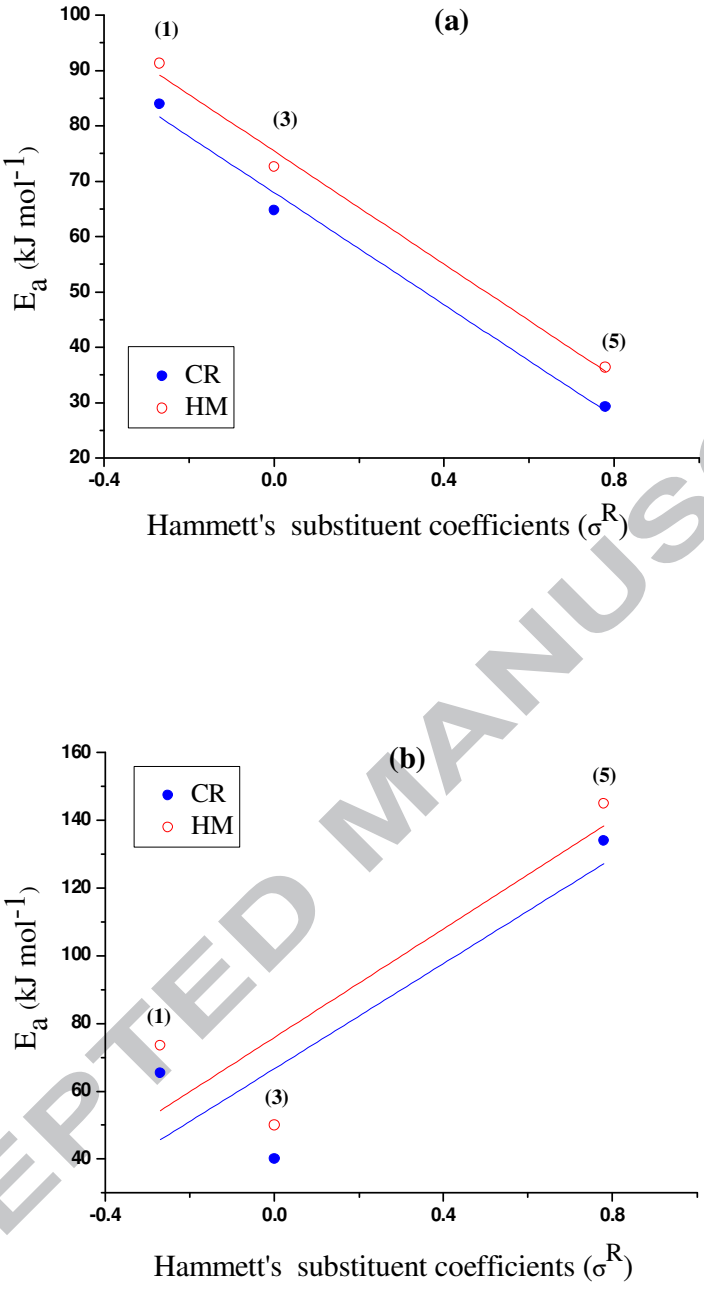

Fig. 11. The relation between E_a and Hammett's substituent coefficients (σ^R) for Cu(II) complexes (**1**, **3** and **5**) a) First stage and b) Second stage.

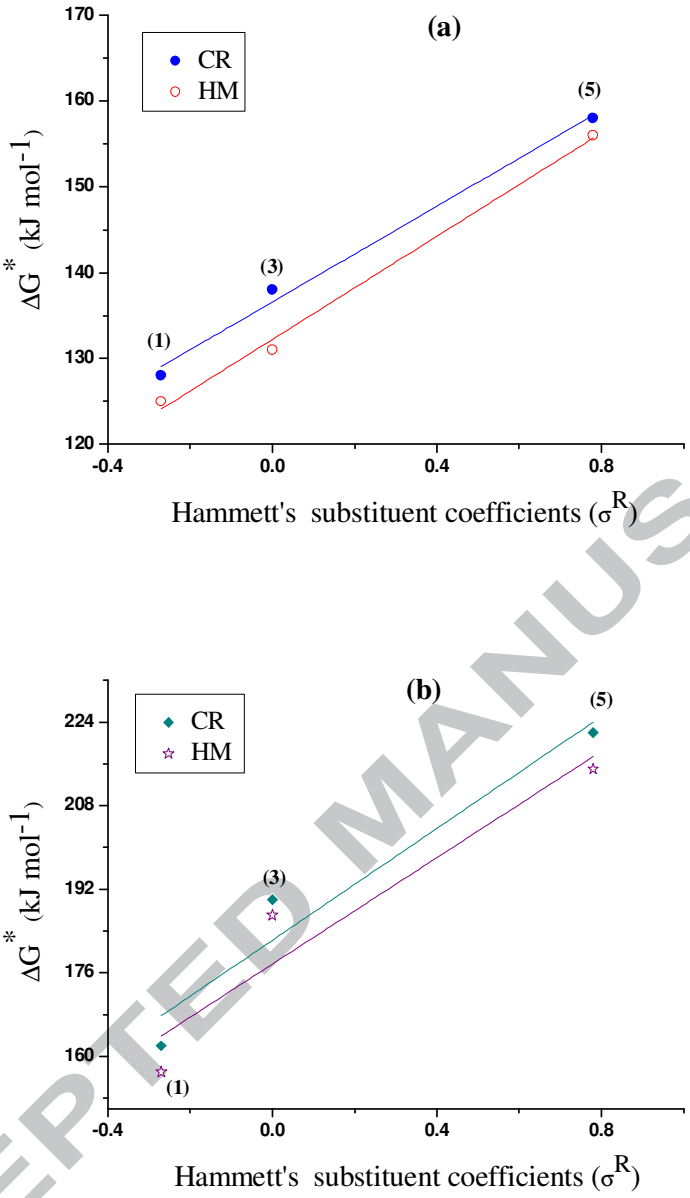

Fig. 12. The relation between ΔG^* and Hammett's substituent coefficients (σ^R) for Cu(II) complexes (**1**, **3** and **5**) a) First stage and b) Second stage.

It was found that the values of Gibbs free energy (ΔG^{*}) for Cu(II) complexes (**1**, **3** and **5**) increase with increasing Hammett's substituent coefficients (σ^{R}), attributed to the fact that the effective charge experienced by the d-electrons increases due to the electron withdrawing *p*-substituent NO_2 while it decreases by the electron donating character of OCH_3.

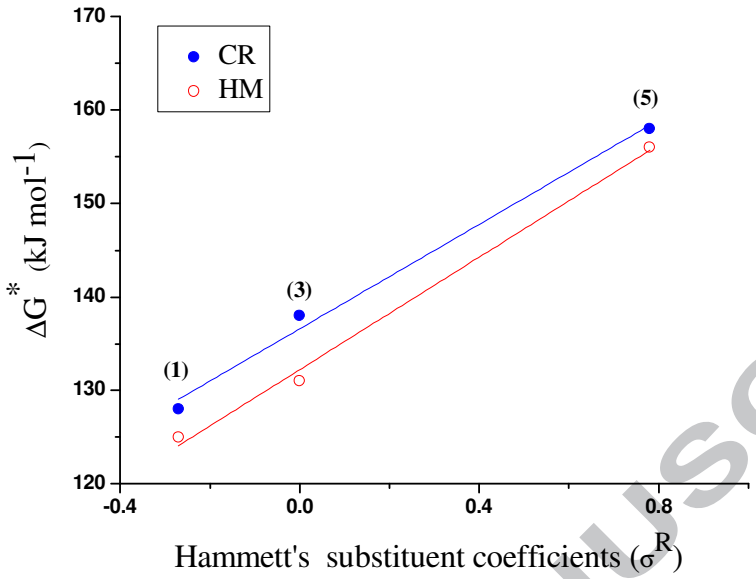

It was found that the values of Gibbs free energy (ΔG^*) for Cu(II) complexes (**1**, **3** and **5**) increase with increasing Hammett's substituent coefficients (σ^R), attributed to the fact that the effective charge experienced by the d-electrons increases due to the electron withdrawing *p*-substituent NO_2 while it decreases by the electron donating character of OCH_3.

- A series of Cu(II) complexes of azo rhodanine derivatives (HL_n) were prepared and characterized.
- It is found that the change of substituent affects the thermal properties of Cu(II) complexes.
- The Cu(II) complexes showed antimicrobial activities against *S. aureus* and *P. italicum*.
- ESR calculations support the characterization of the structures of the complexes geometries.
- Different thermodynamic parameters were discussed.